3

सिंटरन के निशान की जांच हेतु कार्बोनेटेड हाइड्रॉक्सीपेटाइट पर टेराहर्ट्ज-रमन स्पेक्ट्रमदर्शी

सुनीता केडिया[1,2,*], जागृति वी. चव्हान[1], प्रिया यादव[3], जी. श्रीधर[1,2], जे.पे. नीलया[1,2]

[1]लेसर एवं प्लाज़्मा प्रौद्योगिकी प्रभाग, भाभा परमाणु अनुसंधान केंद्र, ट्रांबे, मुंबई-400085, भारत
[2]होमी भाभा राष्ट्रीय संस्थान, अणुशक्तिनगर, मुंबई-400094, भारत
[3]भौतिकी विभाग, के.जे. सोमैया, विद्याविहार, मुंबई-400077, भारत

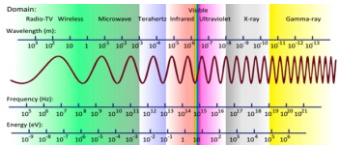

विद्युत-चुंबकीय वर्णक्रम

सारांश

टेराहर्ट्ज-रमन स्पेक्ट्रमदर्शी (टीएचजेड-रमन) एक प्रगत घूर्णन-कंपन स्पेक्ट्रमदर्शिकी तकनीक है जो संरचनात्मक एवं आण्विक उपस्थिति के प्रमाण (अंगुल-छाप) प्रदान कर सकती है। इस कार्य का उद्देश्य रासायनिक रूप से संश्लेषित कार्बोनेटेड एपेटाइट, एक अस्थि खनिज अनुहार, का उच्च तापमान 400, 600, 700 और 800^{0} C पर सिंटर कर अभिलक्षणन करना था। इसकी विशेषता 400^{0} C (सीए-400) पर THz-रमन शीर्ष तीव्रता में एक महत्वपूर्ण वृद्धि शिथिल बंध जल और हाइड्रॉक्सिल समूहों को हटाने से उत्पन्न संरचनात्मक पुनर्गठन है। मध्यवर्ती तापमान (600-700^{0} C) पर, कम तीव्रता और चरम विस्तार कार्बोनेट की कमी, आंशिक अपघटन एवं जालक पुनर्संरचना को इंगित करता है। 800^{0} C पर, टेराहर्ट्ज़ क्षेत्र (<200 cm^{-1}) में अतिरिक्त कंपन विशेषताओं का उद्भव बेहतर क्रिस्टलीकरण और संभावित प्रावस्था परिवर्तन का संकेत देता है। ध्यातव्य है कि, Ca-O कंपन मोड (O-Ca-O) विशेष रूप से टेराहर्ट्ज क्षेत्र में देखे गए और पारंपरिक रमन वर्णक्रमीय सीमा में अनुपस्थित थे, जो निम्न आवृत्ति जालक कंपन के प्रग्रहण में टेराहर्ट्ज-रमन स्पेक्ट्रमदर्शी के महत्व को उजागर करते हैं।

3

Terahertz-Raman Spectroscopy on Carbonated Hydroxyapatite to Investigate the Signature of Sintering

Sunita Kedia[1,2,*], Jagruti. V. Chavan[1], Priya Yadav[3], G. Sridhar[1,2]and J. P. Nilaya[1,2]

[1]Laser & Plasma Technology Division, Bhabha Atomic Research Centre, Trombay-400085, INDIA
[2]Homi Bhabha National Institute, Anushakti Nagar, Mumbai-400094, INDIA
[3]Department of Physics, K. J. Somaiya, Vidyavihar, Mumbai-400077, INDIA

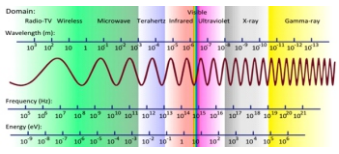

Electromagnetic spectrum

ABSTRACT

Terahertz-Raman spectroscopy (THz-Raman) is an advanced rotational-vibrational spectroscopic technique which can provide structural and molecular fingerprints. This work was aimed to characterize chemically synthesized carbonated apatite, a bone mimicking mineral, sintered at elevated temperatures 400, 600, 700 and 800^{0}C. A significant enhancement in the THz-Raman peak intensity at 400^{0}C is attributed to structural reorganization arising from the removal of loosely bound water and hydroxyl groups. At intermediate temperatures (600-700^{0}C), reduced intensity and peak broadening indicate carbonate loss, partial decomposition and lattice restructuring. At 800^{0}C, the emergence of additional vibrational features in terahertz region (< 200 cm^{-1}) indicates improved crystallinity and possible phase transformation. Notably, Ca-O vibrational modes (O–Ca–O) were observed exclusively in the terahertz region and were absent in the conventional Raman spectral range, highlighting the significance of terahertz-Raman spectroscopy in capturing low-frequency lattice vibrations.

KEYWORDS: *THz-Raman spectroscopy, Rotational-vibrational energy levels, Carbonated apatite, Bone mineral*

**Author for Correspondence: Sunita Kedia*
E-mail: skedia@barc.gov.in

Introduction

Material characterization is of immense significance as it provides an insight into the chemical composition and structural arrangement of the materials which gives further information about bonding, purity, defects, mechanical, biological, thermal, and optical properties. Characteristic information prior to development helps in optimizing design and processing, saving significant time and resources. A range of techniques such as Scanning Electron Microscopy (SEM), X-ray Diffraction (XRD), Fourier Transform Infrared Spectroscopy, X-ray Photoelectron Spectroscopy, and Transmission Electron Microscopy are already in use for this purpose. Among them, Raman spectroscopy is a widely used and a powerful analytical technique based on the inelastic scattering of light, arising from changes in the polarizability of molecules. It provides a unique molecular fingerprint of materials. In this process, the energy of the incident photons, when they get scattered from molecules, undergoes a shift. When the photons lose energy during this interaction, it is termed a Stokes shift, whereas when they gain energy, it is referred to as an anti-Stokes shift (Fig.1a) [1]. Raman spectroscopy can also be used to study phase transition, vibrational rotational modes, glass transition and relaxation processes [2]. A conventional Raman spectrometer is associated with molecular vibration in a spectral range from 200 cm^{-1} to 4000 cm^{-1} and Raman signal in the range of 500 cm^{-1} to 1500 cm^{-1} provides chemical fingerprint of the molecules [3]. In last few decades, Raman spectroscopy at low wavenumbers (< 200 cm^{-1}), also known as Terahertz Raman spectroscopy (THz-Raman), has added an advancement in the analysis technique by providing structural fingerprint of the molecules and gained relevance in the research, Fig.1b [4]. THz-Raman spectroscopy has been used as an advanced vibrational-rotational spectroscopy approach in the range of ~ 0.1 – 10 THz or 3-300 cm^{-1} to probe low-frequency molecular vibrations correspond to hydrogen bonding, lattice vibrations, intermolecular interactions, or phonons that are often invisible in the conventional Raman or IR spectra [5]. The ability to safely and remotely detect unknown materials is an advantage of THz-Raman spectroscopy that is responsible for its wide popularity. Many explosives and hazardous chemicals have strong transition < 6 THz (200 cm^{-1}) regime. Carriere et al. used THz-Raman to fingerprint different polymorphic forms of Carbamazepine with same chemical composition and Ammonium Nitrate, the material commonly used in explosives [6]. Singh et al. used THz-Raman spectroscopy to identify five common nitrogen based high energy organic compounds [7]. Zhang et al. reported THz-Raman spectra of graphite flaks and single walled carbon nanotubes [8]. Carpinteri *et al.* studied mechanical vibration of crystalline lysozyme enzyme in THz-Raman range [9].

Apatite is the primary mineral component of biological hard tissues such as bones and teeth and is extremely important in biomaterials and biomedical engineering [10]. It is a group of calcium phosphate minerals with general formula $Ca_{10}(PO_4)_6(X)_2$ where X can be -OH, -Cl, -F, C etc. Apatite possess hexagonal lattice where phosphate group (PO_4^{3-}) form a tetrahedral structure and calcium ion occupy two distinct crystallographic positions designated as Ca (I) and Ca (II) sites, as shown with blue and red colour, respectively in Fig.1c [11]. Carbonated apatite (CA) which is chemically more similar to natural bone is a modified form in which carbonated ion (CO_3^{2-}) gets substituted into crystal lattice of hydroxyapatite [$Ca_{10}(PO_4)_6(OH)_2$: (HAP)] and alters the physical and chemical properties of the lattice [12]. The CA when sintered to elevated temperature can undergo significant chemical and structural changes due to the thermal instability of carbonate group. Since, selective laser sintering of CA Is employed for scaffold fabrication utilized as implant materials, study of its temperature dependent properties is of great significance.

In this work CA was synthesized by chemical method and characterized using SEM, EDS (energy dispersive x-ray spectroscopy), XRD and Raman spectroscopy. The CA powder was sintered at various elevated temperatures and its corresponding morphology was studied using SEM. Temperature dependent change in THz-Raman spectra were reported in the range of 0.6 cm^{-1} to 3000 cm^{-1}.

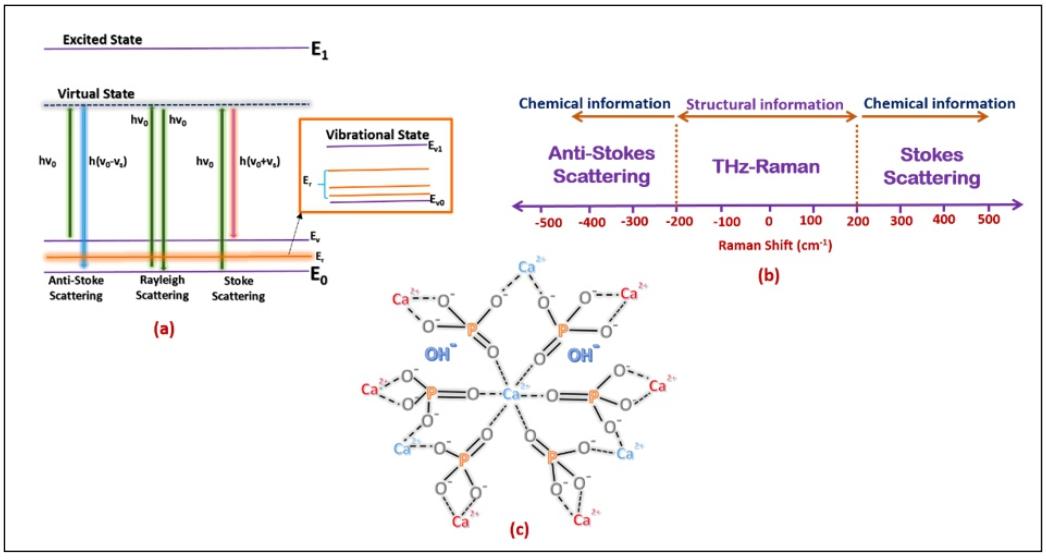

Fig.1: Illustration of typical (a) vibrational and rotation level of a molecule, (b) Terahertz and Raman spectrum range and (c) molecular structure of apatite.

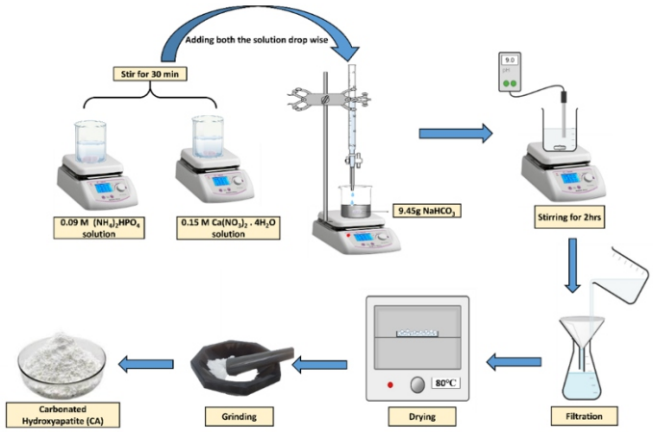

Fig.2: Illustration the steps for synthesis of CA.

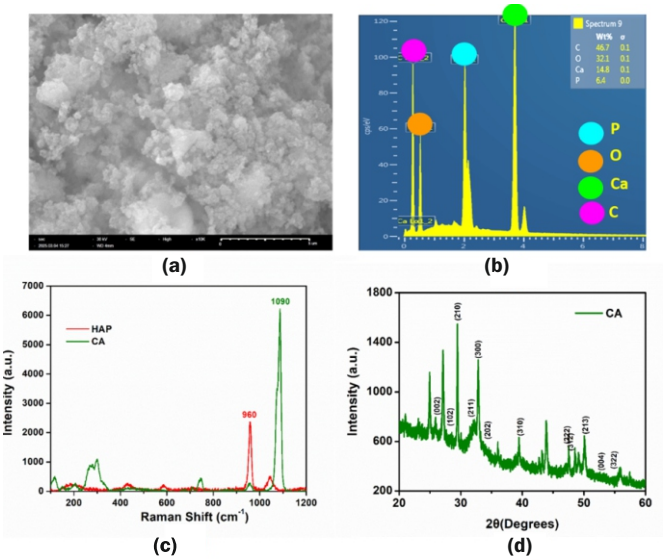

Fig.3: (a) SEM image (b) EDS analysis of as synthesized CA, (c) Raman spectra of HAP and CA (d) XRD of as synthesized CA.

Experiment

For synthesis of CA, about 9.45 g of $NaHCO_3$ was added to 250 ml of distilled water heated at 60°C placed on a magnetic stirrer to prepare bicarbonate mixture. Separately, about 8.85 g of 0.15 M of $Ca(NO_3)_2.4H_2O$ in 250 ml of DI water and 2.97 g of 0.99 M of $(NH_4)_2HPO_4$ in 250 ml of DI water were stirred for 30 min. These two solutions were added into the bicarbonate mixture drop wise. The pH of the mixture was adjusted and maintained at 9 by adding ammonium hydroxide solution. The reaction mixture was continuously agitated at 1000 rpm and 60°C for 2 h. The precipitates was then washed three times with mixture of distilled water and 5% ethanol [13]. The residue was then dried at 80°C for 24 h in an oven and ground to a fine powder to obtain CA. A schematic diagram illustrating the steps of CA synthesis is shown in Fig. 2. For THz-Raman characteristics, CA powder was sintered at elevated temperature of 400°C, 600°C, 700°C and 800°C and sintered samples were termed as CA-400, CA-600, CA-700 and CA-800, respectively. Morphology of CA samples was studied using SEM (S&C 4500 M) and THz-Raman characterization was done in the range of 0.6 cm^{-1} to 3300 cm^{-1} (0.018 to 89 THz) using IndiRAM CTR300C Confocal Micro Raman/PL Spectrometer.

Results and Discussion

Fig.3a shows SEM image of as synthesized CA in which nanostructured powder is clearly visible. In EDS analysis shown in Fig.3b, detection of carbon along with Ca and P without additional impurity confirmed success of carbonation. Raman spectra of as synthesized CA and HAP (for the sake of comparison) are shown in Fig.3c. One can notice that the characteristic peak of HAP at 960 cm^{-1} corresponding to PO_4^{3-} stretching diminished and sharp an intense peak at 1090 cm^{-1} was observed in case of CA. This peak at 1090 cm^{-1} corresponds to the ν_1 symmetric stretching mode of CO_3^{2-} ions in CA [14, 15].This indicated that PO_4^{3-} in HAP lattice was replaced by CO_3^{2-} molecules during the process of carbonization and this is called B-type substitution. Another possible replacement is -OH site in HAP by CO_3^{2-} and that is called A-type substitution [12]. Most of the biological apatites are of B-type CA. Fig.3d shows the XRD data that exhibit typical diffraction peaks at 25.8°, 28.1°, 29.4°, 31.9°, 32.9°, 34.0°, 39.5°, 47.5°, 48.5°, 50.05°, 53.1°, and 55.9° corresponding to (002), (102), (210), (211), (112), (300), (202), (310), (222), (312), (213), (004), and (322) planes of CA respectively(JCPDS 09–0432) [16].

Figs.4a-4d show the SEM images of sintered CA powder where temperature dependent change in morphology is clearly visible. Fig.4e shows the THz-Raman spectra of as synthesized and sintered CA samples. In Raman band from 400 cm^{-1} cm to 1300 cm^{-1}, the characteristic peak of CA the characteristic peak of CA showed a significant increment for CA-400. This could be because at 400°C removal of loosely bound water, hydroxyl group and surface impurity induced structural reorganization and improved detectability of carbonated group [17]. Further, possibility of crystalline order of apatite lattice at this temperature may have enhanced the efficiency of Raman scattering. For CA-600, there is a possibility of carbonated group decomposing and release of CO_2 gas from the lattice structure. This resulted in the reduction of Raman peak intensity at 1090 cm^{-1}. As carbonate content reduces in the structure, the lattice shift towards stoichiometric HAP and therefore, the characteristic peak of PO_4^{3-} stretching of HAP was observed 960 cm^{-1}. On further sintering to 700-800°C, significant decomposition resulted in alteration of Ca/P ratio of apatite and phase transition to β-tricalcium phosphate (β-TCP) [17]. The defects generated during carbonated substitution get removed during sintering at these high temperature and generate more ordered structure [18].

A significant temperature dependent behavior was observed for CA in THz-Raman band (1-10 THz or 0-333 cm^{-1}) which correspond to phonon vibrations that arise due to collective motion of atoms in the crystal lattice (Fig.4e). As synthesized CA that is characterized by broad bands at 3.4 THz, 4.53 THz, 5.13THz, 6.12 THz, 8.00 THz and 8.97 THz indicates poor crystallinity and structural disorder. The CA-400, exhibited two significantly intense sharp peaks centered around

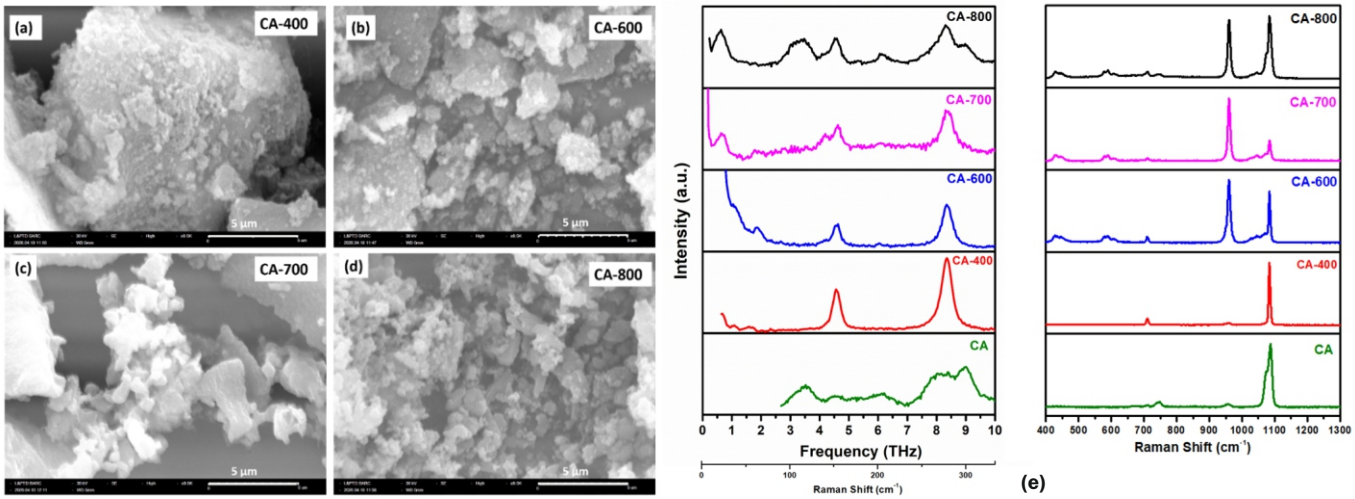

Fig.4: SEM images of (a) CA-400, (b) CA-600, (c) CA-700, (d) CA-800 and (e) THz-Raman spectra of CA, CA-400, CA-600, CA-700 and CA-800.

4.56 THz and 8.33 THz along with low intense peaks at 1.08 THz, 1.59 THz, 2.02 THz, and 2.32 THz. In the intermediate temperatures (600-700^{0}C), reduction in peak intensity and peak broadening indicated structural modification due to loss of carbonated group, decomposition and restructuring. Here the observed THz-Raman bands were at 1.06 THz, 1.85 THz, 2.64 THz, 4.56 THz and 8.33 THz. At 800^{0}C, additional vibrational features appeared in the THz-Raman spectrum, indicated possible phase transformation and modification in lattice dynamics [19]. Surface phonons contributes strongly in low-frequency Raman signals results in bond splitting and appearance of new peaks. It has been reported that the THz-Raman peaks detected < 2 THz (< 70 cm^{-1}) corresponds to translational vibration motion of Ca^{2+} ions. Peaks between 2-6 THz (70-200 cm^{-1}) corresponds to librational (restricted rotational) modes of PO_4 and CO_3 groups. And, the peaks between 6- 10 THz are low energy optical vibration of O-Ca-O bending [20].

Conclusion

The CA powder was successfully synthesized via a simple in-house chemical technique. Superior quality and purity of CA powder was confirmed from EDS, Raman and XRD. The signature of sintering (400–800^{0}C) was systematically investigated using THz-Raman spectroscopy in both the terahertz (0–10 THz) & conventional Raman (400–1300 cm^{-1}) regime. The terahertz regime revealed collective translational and librational motions of Ca^{2+} ions and PO_4/CO_3 units, which are not accessible in the conventional Raman range. Carbonate substitution-induced lattice disorder was evident from peak broadening in the THz spectra for CA-600 and CA-700, providing direct insight into structural dynamics and substitution mechanisms. With increasing sintering temperature, progressive decarbonation, and enhanced crystallinity, were observed. These findings demonstrate that terahertz-Raman spectroscopy serves as a powerful complementary tool for probing low-frequency lattice vibrations and offers enhanced sensitivity for identifying structural evolution in apatite systems.

Acknowledgment

The authors gratefully acknowledge Nayna D Jadhav, ILS, L&PTD for technical help.

Reference

[1] A. Orlando, F. Franceschini, C. Muscas, S. Pidkova, M. Bartoli, M. Rovere, and A. Tagliaferro, “A comprehensive review on Raman spectroscopy applications” Chemosensors 9 (2021) 262.

[2] Y. Qiu, H. Liu, N. Ma, J. Chen, H. Ding, Z. Hu, and D. Zhong, “Variable Temperature Raman Spectroscopy study of the phase transition mechanism in asphalt binders” Energy & Fuels 37 (2023) 10296.

[3] D. B. Menezes, A. Reyer, A. Yüksel, B. B. Oliveira, M. Musso, “Introduction to Terahertz Raman spectroscopy” Spectroscopy Letters, 51 (2018) 438-445.

[4] Q. Zhao, J. Zhang, Y. Jing, J. Xue, J. Liu, J. Qin, Z. Hong, and Y. Du, “Terahertz and Raman vibrational spectroscopy detection and structural analysis of acyclovir hydrate polymorphs” Spectrochimica Acta Part A: Molecular and Bimolecular spectroscopy 338 (2025) 126093.

[5] M. Takahashi, “Terahertz vibrations and hydrogen-bonded networks in crystals” Crystals 4 (2014) 74-103.

[6] J. T. A. Carriere, F. Havermeyer, and R. A. Heyler, “THz-Raman Spectroscopy for Explosives, Chemical and Biological Detection” Proc. Of SPIE 8710 (2013) 87100M-1.

[7] K. Singh, U. Aalam, A. Mishra, N. Dixit, A. Bandyopadhyay, A. Sengupta, “Spectroscopic and imaging considerations of THz-TDS and ULF-Raman techniques towards practical security applications” Optics Express 32 (2024) 1314-1324.

[8] H. Zhang, Q. Yan, J. Tian, L. Wang, “Terahertz Raman Mode Analysis in Graphite Flakes and Single-Walled Carbon Nanotube Aerogels: Experimental and Theoretical Insights” The Journal of Physical Chemistry C, 129 (2025) 11508−11517.

[9] A. Carpinteri, G. Lacidogna, G. Piana, A. Bassani, "Terahertz mechanical vibrations in lysozyme: Raman spectroscopy vs modal analysis" Journal of Molecular Structure 1139 (2017) 222-230.

[10] M. S. Amin, L. K. Randeniya, A. Bendavid, P. J. Martin, E. W. Preston, "Biomimetic apatite growth from simulated body fluid on various oxide containing DLC thin films" Diamond and Related Materials, 21, 2012, 42-49.

[11] S. Markovic, L. Veselinovic, M. J. Lukic, L. Karanovic, I. Bracko, N. Ignjatović, D. Uskokovic, "Synthetical bone-like and biological hydroxyapatites: a comparative study of crystal structure and morphology" Biomedical Materials, 6 (2011) 4.

[12] E. Garskaite, K. A. Gross, S. W. Yang, T. C. K. Yang, J. C. Yang, A. Kareiva, "Effect of processing conditions on the crystallinity and structure of carbonated calcium hydroxyapatite (CHAp)" Royal Society of Chemistry, 16 (2014) 3950–3959.

[13] S. Wang, C. hao, X. Zhao, Y. Guo, H. Song, L. Shen, Z. Zhou, Z. Li, "Application of Three-Dimension Printing Nano-Carbonated-Hydroxylapatite to the Repair of Defects in Rabbit Bone" International Journal of Nanomedicine, 19 (2024) 1667-168.

[14] S. S. Priyadharshini, C. Ragavendran, A. Sherwood, J. R. Ramya, and J. Keithikadatta, "Evaluation od mineral induction ability and cytotoxicity of carbonated hydroxyapatite for pulp tissue regeneration: an in vitro study" Restor Dent Endod 49 (2024) 2234.

[15] J. F. Alves, H. G. M. Edwards, A. Korsakov, and L. F C de Oliveira, "Revisiting the Raman spectra of carbonated minerals" Minerals 13 (2023) 1358.

[16] K. Benataya , M. Lakrat, L.L. Elansari, E. Mejdoubi, "Synthesis of B-type carbonated hydroxyapatite by a new dissolution precipitation Method" Materials Today: Proceedings, 31 (2020) S83-S88.

[17] N. Bohme, K. Hauke, M. Dohrn, M. Neuroth and T. Geisler "High temperature phase transformations of hydroxyapatite and the formation of silicocarnotite in the hydroxyapatite quartz lime system studied in situ and in operando by Raman spectroscopy" Ceramics 57 (2022) 15239.

[18] M. N. M. Syazwan, M. N. A. Fauzi, W. Balestri, Y. Reinwald and B. I. Y. Marliana, "Effectiveness of various sintering aids on the densification and in vitro properties of carbonated hydroxyapatite porous scaffolds produced by foam replication technique" Materialstoday communications 27 (2021) 102395.

[19] J. Kirkham, T. M. Korter, K. Berziņs, C. M. McGoverin, K. C. Gordon, S. J. Fraser-Miller, "Characterization of Variably Substituted Hydroxyapatites Using Low-Frequency Raman Spectroscopy" Crystal Growth & Design, 23, 2023, 5748–5761.

[20] M. Markovic, B. O. Fowler, M. S. Tung, "Preparation and Comprehensive Characterization of a Calcium Hydroxyapatite Reference Material" Journal of Research of the National Institute of Standards and Technology , 109, 2004, 6.